Volume 16 Number 13 1988 Nucleic Acids Research

A selective recognition mode of a nucleic acid base by an aromatic amino acid: L-phenylalanine–7-methylguanosine 5'-monophosphate stacking interaction

Toshimasa Ishida, Mitsunobu Doi and Masatoshi Inoue

Laboratory of Physical Chemistry, Osaka University of Pharmaceutical Sciences, 2-10-65 Kawai, Matsubara, Osaka 580, Japan

Received April 7, 1988; Revised and Accepted May 31, 1988

ABSTRACT

The conformation of 7-methylguanosine 5'-monophosphate (m7GMP) and its interaction with L-phenylalanine (Phe) have been investigated by X-ray crystallographic, ^{1}H-nuclear magnetic resonance, and energy calculation methods. The N(7) methylation of the guanine base shifts m7GMP toward an anti—gauche,gauche conformation about the glycosyl and exocyclic C(4')-C(5') bonds, respectively. The prominent stacking observed between the benzene ring of Phe and guanine base of m7GMP is primarily due to the N(7) quarternization of the guanine base. The formation of a hydrogen bonding pair between the anionic carboxyl group and the guanine base further stabilizes this stacking interaction. The present results imply the importance of aromatic amino acids as a hallmark for the selective recognition of a nucleic acid base.

INTRODUCTION

The study of the interactions between amino acids and nucleotides is important for understanding the ability of a protein to recognize a specific base sequence of nucleic acid.

Four basic interaction modes (1) have been accepted regarding the two molecules: (a) an ionic interaction between a negatively charged phosphate and a positively charged amino acid side chain, (b) a hydrogen bond between polar atoms of a nucleotide and a hydrophobic amino acid side chain, (c) a stacking interaction between a nucleic acid base and an aromatic amino acid side chain, and (d) a hydrophobic interaction between a nucleic acid base and a nonpolar amino acid side chain. Among them, the (b) and (c) interaction modes appear to be most favorable for the specific recognition by an amino acid of a nucleic acid base, because the formation of the hydrogen-bonded pair or aromatic π-π interaction can select the most suitable partners among various molecular combinations.

In order to fully understand the biological importance of this specific interaction, therefore, it is necessary to know the binding mechanism at the atomic level. In contrast to the hydrogen-bonded interaction, a clear-cut presentation of the stacking interaction is very meager in the crystalline state. This is primarily due to the interaction force that is not strong enough to overcome the external effects such as crystal packing, although the importance of this interaction has been fully exemplified in the solution state (2,3).

In this paper, which describes the L-phenylalanine (Phe)—7-methylguanosine 5'-monophosphate (m7GMP) interaction, we want to emphasize that the positive charge on the nucleic acid base significantly strengthens the stacking interaction with the aromatic amino acid. Furthermore, the study of the interaction of m7GMP with an aromatic amino acid might help to understand the specific recognition between the cap terminal structure of eukaryotic mRNA where m7GMP is a constitutent and the cap binding protein (CBP) which contains many aromatic amino acid residues (4,5). This paper deals with the conformation of m7GMP and its interaction characteristics with the Phe molecule studied by X-ray crystallographic, ^{1}H-nuclear magnetic resonance (NMR) and theoretical energy calculation methods; preliminary X-ray results have been reported (6).

MATERIALS AND METHODS

Preparation of m7GMP—Phe complex crystals

m7GMP formate was synthesized by the methylation of GMP with dimethylsulfate according to the previously described procedure (7), and converted to the OH form by using a column of Amberlite IRA-401 anion-exchange resin. After many attempts to cocrystallize m7GMP with Phe, transparent thin-layered crystals were obtained from an equimolar mixture dissolved in 70% aqueous propanol by slow evaporation at room temperature. Absorption spectra, electrophoresis and water content showed that the crystals consist of a 1:1 complex of both the molecules and contain six water molecules per complex pair. The crystals were very fragile and rapidly became opaque (amorphous) upon exposure to air. Furthermore, the crystals were highly disordered along the

Table 1. Crystal data for m7GMP–Phe complex

Chemical formula	$C_9H_{11}NO_2 \cdot C_{11}H_{16}N_5O_8P \cdot 6H_2O$
Mr	650.53
Crystal system	monoclinic
Space group	$P2_1$
Cell constants	
a , Å	13.987(6)
b , Å	7.274(2)
c , Å	15.329(7)
β , deg	104.25(3)
Volume, Å^3	1512(1)
Z	2
Dm , g/cm^3	1.419(7)
Dx , g/cm^3	1.429
μ(Cu Kα), cm^{-1}	15.04
F(0 0 0)	688
No of collected reflections	2816
No of $F_o^2 > 3\sigma(F_o)^2$	1844

longest axis. Single crystals with dimensions of approx. 0.05 x 0.1 x 0.4 mm were prepared by cutting larger crystals under the polarizing microscope and were sealed in glass capillaries in the presence of some mother liquor.

X-ray crystal analysis

The crystal data are given in Table 1. X-ray intensity data up to 2θ=130° were measured on an automated Rigaku AFC-5 diffractometer with graphite-monochromated Cu Kα radiation using the ω-2θ scan technique. The scan speed was 1°/min and the background was counted for 5s at both extremes of every reflection peak. The intensities of four standard reflections, which were measured every 50 reflection intervals throughout the data collection, decreased smoothly with X-ray radiation time. When they decreased below 0.8 of the initial values, a new crystal was used for the data collection. The measured intensities were corrected for this instability, and also for Lorentz and polarization effects. No correction was made for the absorption and extinction effects because of the small crystals used.

The structure solution by the heavy atom method failed because of the large thermal motion of the phosphorus atom, but was finally successful with a combination of the Patterson vector search and direct methods (8). Due to the poor quality of the crystals, the intensity data were limited and consequently the non-hydrogen atomic parameters were refined by a full-matrix least-squares method with isotropic temperature factors. The ideal positions of hydrogen atoms were calculated and included only in the calculations of structure factors. The function minimized was $\Sigma w(|Fo|-k|Fc|)^2$, where $|Fo|$ and $|Fc|$ are the amplitudes of observed and calculated structure factors, respectively. In the final refinement, $w=1.0/[\sigma(Fo)^2+0.689|Fo|-0.006|Fo|^2]$ and k (scale factor) of 0.218 were used for 1844 reflections of $Fo^2 > 3\sigma(Fo)^2$, where $\sigma(Fo)^2$ is the standard deviation of the reflection intensity based on counting statistics. The final $R(=\Sigma||Fo|-|Fc||)/\Sigma|Fo|)$, $Rw(=[\Sigma w(|Fo|-|Fc)^2/\Sigma w|Fo|^2]^{1/2})$ and S, the goodness of fit, $(=[\Sigma w(|Fo|-|Fc|)^2/(N-P)]^{1/2})$ were 0.15, 0.10 and 1.07, respectively, where N is the observed reflection number used for refinement and P is the number of variable (=173) in the refinement. For all crystallographic computations, the UNICS programs (9) were used, and the atomic and anomalous scattering factors were taken from the International Tables for X-ray Crystallography (10).

^{1}H-NMR measurements

^{1}H-NMR spectra were measured on a Varian XL-300 (300 MHz for proton; Fourier transform mode) spectrometer equipped with the temperature-control accessory (accuracy to $\pm 1°$ C). Chemical shifts were measured from an internal standard DSS (2,2-dimethyl-2-silapentane-5-sulphonate). The samples were lyophilized three times in 99.8% D_2O, and finally dissolved in deuteriated 25mM phosphate buffer (pD=6.7). The sample concentrations were determined by dry weight and then adjusted to the desired values by dilution. The peak assignments were made by nuclear decoupling and by comparison of related spectra.

The association constant (K) was estimated under the condition of [m7GMP]<<[Phe] using the following Scatchard equation (7):

$$(\delta - \delta_o)/Bo = -K[(\delta - \delta_o) - (\delta_c - \delta_o)],$$

where δ_o and δ are the chemical shifts of a proton of m7GMP in

the absence and presence of Phe ,respectively, and δ_c is the chemical shift of the same proton of m7GMP completely complexed with the Phe molecule. B_o is the concentration of Phe.

Conformational energy calculations of m7GMP as a function of ribose puckering

The total energy for each conformer was calculated as the summation of steric (Lennard-Jones potential), electrostatic (Coulombic), torsional and intramolecular hydrogen bond energies. The net charge of each atom used for the electrostatic energy calculation was obtained from CNDO/2 calculations. The programs and parameters necessary for these calculations were available from the CHEMLAB-II system (11). The dielectric constant was taken as 4.0, close to the experimental value for biomolecules in polar media. The atomic parameters of m7GMP for the calculations were taken from the crystal structure of the m7GMP—tryptamine complex (12), because these data are far superior to the present ones in their accuracy. The atomic parameters for various ribose puckerings were constructed as a function of the pseudorotation phase angle P, according to the equations defining each torsion angle in the furanose ring (13,14). For energy minimization, each torsion angle about glycosyl, exocyclic C(4')-C(5'), C(5')-O(5') and O(5')-P bonds was optimized as a variable parameter by the Powell algorithm (15), where these torsion angles are defined by χ[C(4)-N(9)-C(1')-O(4')], γ[C(3')-C(4')-C(5')-O(5')], β[C(4')-C(5')-O(5')-P] and α[C(5')-O(5')-P-O(1)P], respectively (see Fig.1 for the atomic numbering). Starting torsion angles for energy minimization were taken as follows: χ= 54 and 216°, γ= 54, 180 and 288°,β=180° and α=90 , 180 and 270°. These values are selected from the statistical distribution of nucleosides and nucleotides (1). Minimization was carried out by parabola approximation with 4° intervals, and no angle was permitted to vary by more than 12° at any step.

All the numerical calculations were carried out on a Micro VAX II computer at the Computation Center of Osaka University of Pharmaceutical Sciences. The tables of the final atomic parameters, observed and calculated structure factors, hydrogen bond distances observed in crystal structure, and minimized torsion angles and their conformational energies for each phase angle of m7GMP are available on request.

RESULTS AND DISCUSSION

Molecular conformation in crystal structure

Owing to the relatively low accuracy of the X-ray crystal structure analysis, the ionic states of Phe and m7GMP molecules were not unequivocally determined. However, the hydrogen bonding modes found in the crystal structure (discussed later) suggest that Phe occurs in a zwitterionic state, and the phosphate group of m7GMP is in a monoanionic form. The molecular conformations of Phe and m7GMP in the crystal are shown in Fig. 1, and the selected torsion angles are listed in Table 2.

Phe molecule. The respective orientations of carboxyl and amino groups are in the trans and cis positions with respect to the benzene ring. As stated in a review (16), this conformation belongs to one of the energetically stable forms of Phe ($\chi^1 = \sim \pm 60°$, $\chi^2 = \sim \pm 90°$).

m7GMP molecule. The rotational position of the base relative to the ribose ring is in the anti region ($\chi = -103°$). The ribose puckering is describable as a C2'-endo envelope form; its pseudorotation phase angle P and the maximum torsion angle ν_{max} are 156° and 25°, respectively. The intimate mutual correlation

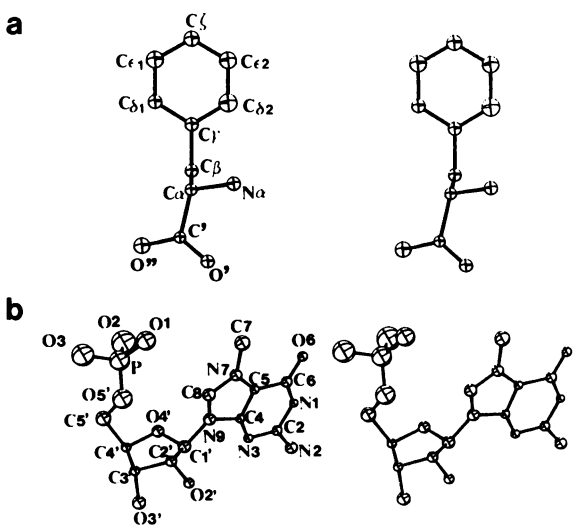

Figure 1. Spectroscopic views of the observed conformations of Phe(a) and m7GMP(b). Thermal ellipsoids are drawn at the 30% probability level. The atomic numberings are also shown.

Table 2. Selected torsion angles (in degrees)

Phe		
ψ	:Nα-Cα-C'-O'	169(2)
χ^1	:Nα-Cα-Cβ-Cγ	-72(2)
χ^{21}	:Cα-Cβ-Cγ-Cδ1	-85(2)
m7GMP		
χ	:C(4)-N(9)-C(1')-O(4')	-103(2)
ν_0	:C(4')-O(4')-C(1')-C(2')	-23(2)
ν_1	:O(4')-C(1')-C(2')-C(3')	32(2)
ν_2	:C(1')-C(2')-C(3')-C(4')	-29(2)
ν_3	:C(2')-C(3')-C(4')-O(4')	18(2)
ν_4	:C(3')-C(4')-O(4')-C(1')	3(2)
P	phase angle of pseudo-rotation	156
ν_{max}	max amplitude of pseudo-rotation	25
δ	:O(3')-C(3')-C(4')-C(5')	148(2)
γ	:C(3')-C(4')-C(5')-O(5')	65(3)
β	:C(4')-C(5')-O(5')-P	155(3)
α	:C(5')-O(5')-P-O(1)	-177(4)

between the base orientation and the ribose puckering is known: the (χ,P) energy profile for purine ribonucleosides (17) shows the most stable region for anti—C2'-endo conformation. This form is just what was found for this nucleotide, implying that the observed molecular conformation of m7GMP is not affected by external factors such as crystal packing forces. The orientations about the exocyclic C(4')-C(5') and C(5')-O(5') bonds take the gauche,gauche(g,g) and trans conformations, respectively, and are also in the energetically favored region (18). The short contact(=3.43(4) Å) between the C(8) and O(5') atoms appears to stabilize the g,g and anti orientations about the C(4')-C(5') and glycosyl bonds by the C(8)-H...O(5') hydrogen bonding interaction.

Solution conformation of m7GMP

The anti—C2'-endo—g.g conformation of m7GMP has also been observed in the complex crystal of m7GMP—tryptamine (12), and seems likely to be a dominant feature of m7GMP in the solid state. This is in conspicuous contrast to the solution confor-

Table 3. Chemical shifts($\delta_{H1'}$), coupling constants($J_{1'2'}$) and ribose puckering populations of m7GMP and GMP as function of Phe concentration at 30°C[a,b]

compound	$\delta_{H1'}$/ppm	$J_{1'2'}$/Hz	C3'-*endo*(%)
0.01M m7GMP	6.071	3.8	60
+ 0.025M Phe	6.062	3.9	59
+ 0.075M Phe	6.049	3.5	63
+ 0.150M Phe	6.034	4.0	58
+ 0.300M Phe	6.019	3.5	63
0.01M GMP	5.922	6.3	35
+ 0.025M Phe	5.917	5.8	40
+ 0.075M Phe	5.907	6.3	35
+ 0.150M Phe	5.897	6.0	38
+ 0.300M Phe	5.879	6.1	37

[a]Estimated standard error is ±0.001ppm for chemical shift, and ±0.3Hz for coupling constant.

[b]L-Phenylalanine methylester, instead of Phe, was used because of the solubility.

mation, in which the preference of the C3'-endo ribose puckering has been reported (7,19,20), although the anti and g,g conformations about the glycosyl and C(4')-C(5') bonds are comparable to the solid state and probably stabilized by electrostatic interactions between the positively charged N(7)-methylated guanine base (m7G) and the negatively charged phosphate group. Therefore, the C2'-endo ribose puckering observed in the crystal structure may be due to the interaction with the Phe molecules. In order to ascertain this possibility, the ribose puckering of m7GMP in a phosphate buffer solution (pD=6.7) was investigated by ^{1}H-NMR measurements. The results are given in Table 3.

The ribose puckering can be treated as a C2'-endo⇌C3'-endo equilibrium state. In this assumption, the population distribution of C3'-endo ribose puckering can be estimated from the widely accepted equation (21):

$$\text{C3'-endo (\%)} = 100 \times [\, J_{3'4'}/(J_{1'2'} + J_{3'4'})],$$

where the standard sums of 9.5 Hz and 9.65 Hz for $J_{1'2'} + J_{3'4'}$ were used for m7GMP and GMP, respectively (20). As is obvious from Table 3, m7GMP prefers to take a C3'-endo ribose puckering

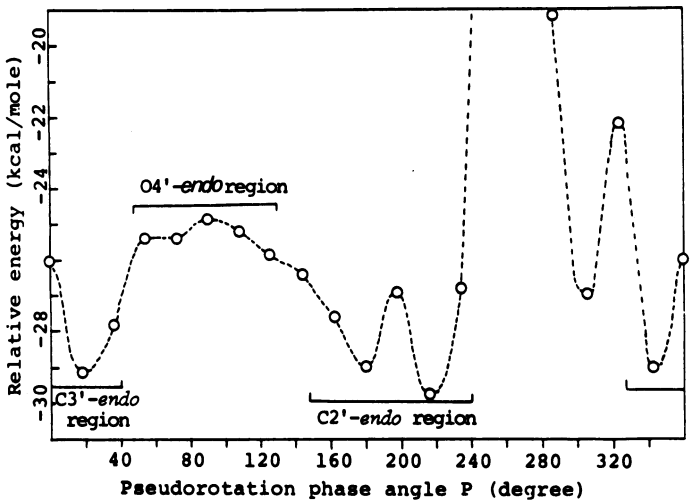

Figure 2. Variation of m7GMP total energy as a function of pseudorotation phase angle P.

rather than C2'-endo one, while GMP shows a reverse preference. Neither ribose puckering of m7GMP nor GMP is significantly affected by the presence of the Phe molecule, although the ring stacking interaction with Phe causes a noticeable up-field shift of H(1') proton. A similar bahaviour has also been observed in the m7GMP—tryptophan system (7). Judging only from this result, N(7) methylation of GMP appears to cause a significant shift in ribose pucker toward the C3'-endo form.

The question remains why the m7GMP ribose puckering is different in the solid state and solution. Since the molecular conformation of m7GMP in the cap terminus is certainly important for the specific recognition by CBP, this question led us to the conformational analysis of m7GMP by energy calculations.

Conformational analysis of m7GMP as a function of the ribose pseudorotation phase angle

The variation of total energy with pseudorotation phase angle P is shown in Fig. 2. Open circles for each P value in this figure give the energy value of the most stable conformer.

Similar to a nucleotide with uncharged base(14), m7GMP shows energetic instability in the region of P=240 - 290°, and a modest energy barrier (∿4kcal/mole) exists for O4'-endo pucker region

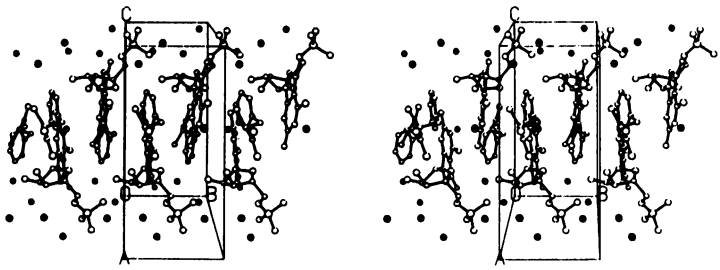

Figure 3. Stereoscopic drawing of the m7GMP—Phe complex crystal structure. The filled circles represent water molecules of crystallization.

(P=60 - 120°) between the two favored ribose puckering states C2'-endo (P=140 - 240°) and C3'-endo (P=0 - 40° and 300 - 360°) regions in a broad sense. There are five kinds of local energy minima (P=18°, 180°, 216°, 306° and 342°). They show nearly the same stability, except for P=306° (C1'-endo pucker), and allow considerable conformational freedom for χ, γ, β and α torsion angles; many stable conformers (-28 — -29 kcal/mole) with different torsion angles have been obtained. It is interesting to note that the energetically metastable conformations with P=60° — 160° all favor the syn orientation about the glycosyl bond (χ=50° — 70°).

This conformational analysis showed no energetic preference for the C(2')-endo ribose puckering of m7GMP. Therefore, we conclude that the difference of the m7GMP ribose puckering observed between the solid and solution states is largely due to the external environment. The solution conformation of m7GMP especially would be influenced by solvation effects. On the other hand, the N(7)-methylation of guanine base strengthens the intramolecular C(8)-H(8)$^{\delta+}$...O(5')$^{\delta-}$ interaction, causing the preference for anti, g,g orientations of χ and γ torsion angles; the net charges of H(8) and O(5') atoms are 0.0296e and -0.3087e for GMP, and 0.0866e and -0.3275e for m7GMP, respectively.

Molecular packing and hydrogen bonds in the m7GMP—Phe complex crystal

A stereoscopic drawing of the molecular packing is illustrated in Fig 3. A characteristic feature is the extensive stacking of aromatic rings, in which guanine and benzene rings

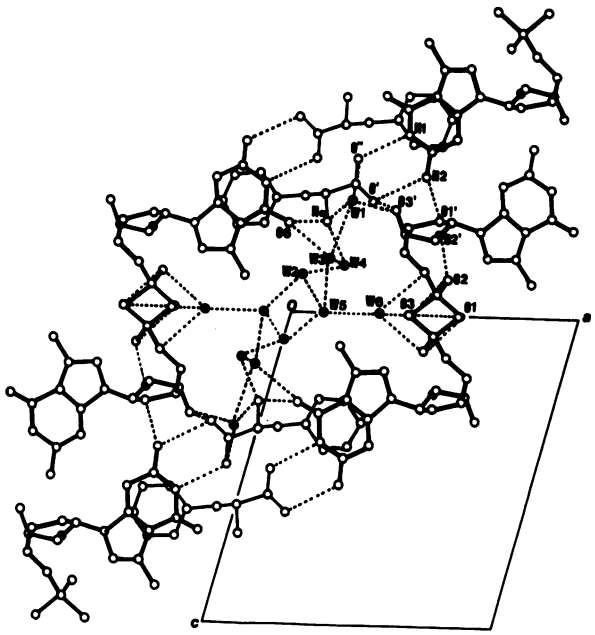

Figure 4. Hydrogen bonds formed in the complex crystal, viewed along the b-axis. Dotted lined show possible hydrogen bonds. Filled circles represent waters of crystallization.

alternate, and pile up along the b-direction. The ribose and phosphate groups of m7GMP and the amino acid moiety of Phe jut out from the layers. The water molecules of crystallization are located between these hydrophilic, charged groups, and stabilize the molecular packing of m7GMP—Phe complex via hydrogen bond formations. The hydrogen bonds formed in the crystal structure are shown in Fig. 4.

Characteristic hydrogen bonds between carboxyl group and guanine base. The carboxyl anion of Phe and the m7G base are linked with each other by two N(1)-H...O'[2.87(3)Å] and N(2)-H...O"[2.79(3)Å] hydrogen bonds. This kind of hydrogen-bonded pairing has also been observed in the 7-methyl-9-ethylguanine—indole-3-acetic acid complex crystal(22) and in the solution state of guanine—carboxylate complex (23). Since guanine is the only base possessing two donor groups which can simultaneously hydrogen-bond with the ionized carboxyl group, this hydrogen-bonded pairing provides a good means for the selective interaction

mode of an ionized glutamic or aspartic amino acid side chain with the guanine base.

The phosphate groups, in which the O(1)P atom probably has a hydrogen atom, as judged from the hydrogen bonding mode, are assembled around a diad screw axis, and form a cylindrical column along the b-axis. They are connected by O(1)P...O(2)P[3.09(6)Å] and O(1)P...O(3)P[2.76(5)Å] hydrogen bonds and O(2)P...O(3)P[3.24 (6)Å] short contact interactions. The Nα atom of Phe is tetrahedrally hydrogen-bonded to O(6), O(1)W and O(6)W atoms [2.76(2), 2.85(3) and 2.76(3)Å], respectively , suggesting that this amino group occurs in the $-NH_3^+$ form.

Extensive hydrogen bond network of water molecules. A relatively large channel is formed around the b-axis by the molecular packing of m7GMP and Phe. This is a major reason why these complex crystals are very fragile and quickly change to an opaque and amorphous state upon exposure to air. Six water molecules of crystallization per complex pair occupy this space, and stabilize the crystal structure. The oxygen atom of each water molecule, as an electron donor or acceptor, participates in three to four hydrogen bonds.

Stacking interaction between m7GMP and Phe molecules

Figure 5 shows a stereoscopic view of the stacking mode between the molecules, where the two up-and-down stacked benzene rings of Phe sandwiching the m7GMP are projected perpendicular (Fig.5a) and parallel (Fig.5b) to the m7G base. The mean interplanar spacings are 3.39 and 3.67 Å for the upper and lower stacking pairs, respectively, and the dihedral angles are 33(1)° for both the pairs. The interplanar spacings close to van der Waals separation distance (3.4 Å) and the relatively large deviation from parallel stacking indicate that these interactions are mainly stabilized by van der Waals forces; the stabilization energy by stacking formation (12) is estimated to be -35.3 kcal/mole for the lower pair and -38.3 kcal/mole for the upper one in Fig.5.

It is well recognized that dipole, electrostatic and molecular orbital interactions are largely responsible for the stacking formation of two interacting molecules. However, in the formation of the present stack, the dipole-dipole interaction between the

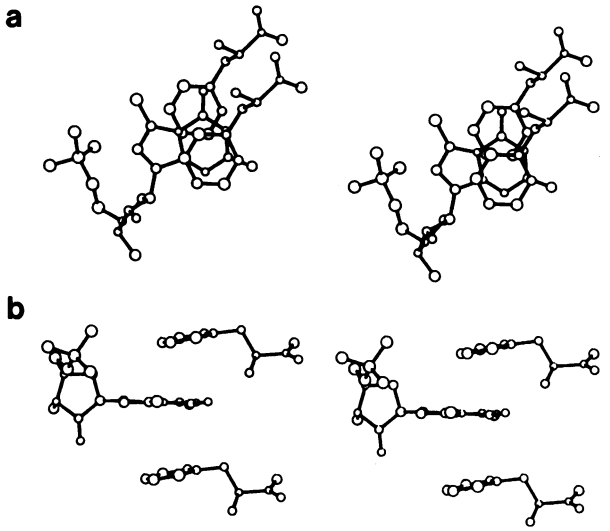

Figure 5. Stereoscopic drawing of stacking interaction modes between m7GMP and Phe molecules

two aromatic rings appears not to be important, because respective dipole moments of m7G base (0.865 debye for 7,9-dimethylguanine) and benzene ring (0.197 debye for 1-methylbenzene) are both small, and their directions are almost at right angles, indicating no dipole-dipole interaction. On the other hand, the electrostatic interactions are likely to be important for stabilizing the stacking. The positive charge caused by the N(7)-methylation is not located on the N(7) atom but spread over the whole guanine base, consequently strengthening the electrostatic interaction with the π electrons of the benzene ring. The major force stabilizing the stacking interaction, however, is the molecular orbital interaction, especially the interaction between the HOMO (highest occupied molecular orbital) of the benzene ring and the LUMO (lowest unoccupied molecular orbital) of m7G base. The N(7)-methylation of the guanine base causes a significant reduction of its LUMO energy (89.3 kcal/mole for 9-methylguanine and -74.8 kcal/mole for 7,9- dimethylguanine). This means that the N(7)-methylation facilitates the interaction with the HOMO of benzene ring by 164.1 kcal/mole. The importance of HOMO—LUMO interaction

for the stacking formation has previously been discussed with other systems (12,24).

Stacking ability of aromatic amino acids with m7GMP. It is of interest to consider which aromatic amino acid among tryptophan, tyrosine and Phe has the best stacking ability with m7GMP. The stacking interaction for the tryptophan—m7G system in the crystalline state has been reported (12); the indole ring of the tryptophan side chain interacts with the m7G base with almost parallel alignment and 3.2 - 3.4 Å interplanar spacing. These stacking parameters show that the indole ring is much superior to the benzene ring of Phe for stacking with m7GMP. The same conclusion has been drawn from ^{1}H-NMR measurements in solution. The application of the Scatchard equation (see experimental section) to the data in Table 3 provides the association constants (K) of 4.66 and 2.02 l/mole for m7GMP—Phe and GMP—Phe complexes, respectively. On the other hand, respective K's of 21.8 and 15.8 l/mole have been reported for m7GMP—tryptophan and GMP—tryptophan complexes(7). Although the stacking parameters concerning the tyrosine—m7GMP interaction are not available at present, we conclude from the π electron-donating ability of each aromatic amino acid (25) that the stacking ability with m7GMP decrease in the order:

tryptophan > tyrosine > phenylalanine

Biological significance in m7GMP—aromatic amino acid stacking interaction

Although the stacking interaction has proven to be an important factor of nucleic acid and protein interaction, the attractive force itself is quite weak and there are very few clear-cut crystallographic model representations of the naturally occurring nucleic acid base—aromatic amino acid system. This may be largely due to the relationship of the energy difference between the HOMO of the aromatic amino acid and the LUMO of the nucleic acid base. As exemplified in the present study, however, the quaternization of the guanine N(7) atom by protonation, methylation or alkylation brings the LUMO energy of the base close to the HOMO energy of the aromatic amino acid, and consequently strenghtens the stacking interaction between both molecules significantly. Because of the high nucleophilicity of the guanine

N(7) atom, the protonation of this atom is likely to take place under acidic or neutral condition. Indeed, X-ray crystal analyses of neutral nucleic acids have often shown the protonated state of the guanine N(7) atom (26). On the other hand, it is well-known that the stacked bases in nucleic acid destack if the base is protonated or alkylated. Therefore, the present results strongly suggest that the aromatic amino acids in proteins can become the hallmarks for the selective recognition with nucleic acid. The repair of alkylated, and consequently damaged nucleotides in nucleic aicds may be achieved *via* the hallmark ability of aromatic amino acids which exist in various DNA repair enzymes.

On the other hand, the present results also shed light on the problem of how CBP can specifically recognize the mRNA cap structure. The cDNA for CBP has shown the existence of many aromatic and acidic amino acids in the protein (5). As can be seen in Fig.4, a combination of stacking interactions by aromatic amino acids and the hydrogen-bonded pairing by acidic amino acid side chains with the m7G base would confer the recognition specificity for the cap termical structure.

It is of interest to say that the present interactions between the guanine base and amino acid are very similar to those in ribonuclease T_1—2'GMP complex (Arni *et al*, unpublished results): guanine base is stacked between two tyrosine aromatic rings(Tyr42 and Tyr45), and hydrogen bonds are formed between guanine N(1), N(2) and the carboxylate oxygens of Glu46 side chain and between mainchain NHs of Tyr45 and Asn44 and guanine O(6). Therefore, this interaction mode would be responsible for the selective recognition of guanine base by protein.

ACKNOWLEDGEMENT

This work was supported by Grants-in-Aid for Scientific Research from the Ministry of Education, Science, and Culture, Japan (No.61571037). The authors are very grateful to Prof.Dr. W.Saenger for providing the interaction data between ribonuclease T_1 and 2'GMP and for helpful discussions.

REFERENCES

1. Saenger,W. (1984) Principles of Nucleic Acid Structure, Spring-Verlag, New York.

2. Hélène,C. and Maurizot,J.C. (1981) CRC Crit.Rev.Biochem. 10, 213-258.
3. Hélène,C. and Lancelot,G. (1982) Prog.Biophys.Mol.Biol. 39, 1-68.
4. Rychlik,W., Gardner,P.R., Vanaman,T.C. and Rhoads,R.E. (1986) J.Biol.Chem. 261, 71-75.
5. Rychlik,W., Domier,L.L., Garner,P.R., Hellmann,G.M. and Rhoads,R.E. (1987) Proc.Natl.Acad.Sci.USA. 84, 945-949.
6. Ishida,T., Kamiichi,K., Kuwahara,A., Doi,M. and Inoue,M. (1986) Biochem.Biophys.Res.Commun. 136, 294-299.
7. Kamiichi,K., Doi,M., Nabae,M., Ishida,T. and Inoue,M. (1987) J.Chem.Soc.Perkin.Trans.2, 1739-1745.
8. Sheldrick,G.M. (1985) In Sheldrick,G.M., Kruger,C. and Goddard,R. (eds), Crystallographic Computing 3, Oxford Univ. Press, New York, pp.175-189.
9. The Universal Crystallographic Computing System-Osaka (1979) Library of Programs, Computing Center, Osaka Univ.
10. International Tables for X-ray Crystallography (1974) Kynoch Press, Birmingham, Vol.IV. pp99, 149.
11. CHEMLAB-II (1986) A Molecular Modelling Software System, Molecular Design Ltd., California.
12. Ishida,T., Doi,M., Ueda,H., Inoue,M. and Sheldrick,G.M. (1988) J.Am.Chem.Soc. 110, 2286-2294.
13. Altona,C. and Sundaralingam,M. (1972) J.Am.Chem.Soc. 94, 8205-8212.
14. Levitt,M. and Warshel,A. (1978) J.Am.Chem.Soc. 100, 2607-2613.
15. Powell,M.J.D. (1964) Comput.J. 7, 155-162.
16. Cody,V. (1985) In Barrett,G.C. (ed), Chemistry and Biochemistry of the Amino Acids, Chapman and Hall, London, pp.625-653.
17. Saran,A., Perahia,D. and Pullman,B. (1973) Theor.Chim.Acta 30, 31-44.
18. Saran,A., Pullman,B. and Perahia,D. (1973) Biochim.Biophys. Acta 299, 497-499.
19. Hickey,E.D., Weber,L.A., Baglioni,C., Kim,C.H. and Sarma,R.H. (1977) J.Mol.Biol. 109, 173-183.
20. Kim.C.H. and Sarma,R.H. (1978) J.Am.Chem.Soc. 100, 1571-1590.
21. Davies,D.B. and Danyluk,S.S. (1974) Biochemistry 13, 4417-4434.
22. Ishida,T., Katsuta,M., Inoue,M., Yamagata,Y. and Tomita,K. (1983) Biochem.Biophys.Res.Commun. 115, 849-854.
23. Lancelot,G. and Hélène,C. (1977) Proc.Natl.Acad.Sci.USA. 74, 4872-4875.
24. Ishida,T., Shibata,M., Fujii,K. and Inoue,M. (1983) Biochemistry 22, 3571-3581.
25. Pullman,B. and Pullman,A. (1958) Proc.Natl.Acad.Sci.USA. 44, 1197-1202.
26. Emerson,J. and Sundaralingam,M. (1980) Acta Crystallogr. Sect.B. B36, 1510-1513.